

COMPUTERIZED ANALYSIS OF MRI FOR THE DIAGNOSIS OF AUTISM

WILLIAM ANDRÉS CANCINO REY

UNIVERSIDAD INDUSTRIAL DE SANTANDER  
FACULTAD DE INGENIERÍAS FISICOMECÁNICAS  
ESCUELA DE INGENIERÍAS  
ELÉCTRICA, ELECTRÓNICA Y DE TELECOMUNICACIONES  
BUCARAMANGA  
2022

COMPUTERIZED ANALYSIS OF MRI FOR THE DIAGNOSIS OF AUTISM

WILLIAM ANDRÉS CANCINO REY

A work submitted in partial fulfillment of the requirements for the degree of  
Electronic Engineer

Director

Said Pertuz, PhD

UNIVERSIDAD INDUSTRIAL DE SANTANDER  
FACULTAD DE INGENIERÍAS FISICOMECÁNICAS  
ESCUELA DE INGENIERÍAS  
ELÉCTRICA, ELECTRÓNICA Y DE TELECOMUNICACIONES  
BUCARAMANGA  
2022

## **AGRADECIMIENTOS**

A mis padres, Mercedes y Andelfo, por los consejos y el apoyo incondicional que siempre me han brindado. En cada momento fueron esa voz que me alentaba a continuar.

A mis hermanos, Andel y Camilito, quienes son la inspiración de este proyecto y me motivan ser mejor cada día. Además, me recuerdan que siempre hay que intentarlo sin importar cuan complejas sean las circunstancias.

A mi director de proyecto, Said Pertuz, por su paciencia, confianza y los valiosos conocimientos aportados durante este tiempo.

## CONTENTS

	<b>pág.</b>
<b>INTRODUCTION</b>	<b>9</b>
<b>1. OBJECTIVES</b>	<b>15</b>
1.1. General objective	15
1.2. Specific objectives	15
<b>2. MATERIALS AND METHODS</b>	<b>16</b>
2.1. Dataset and preprocessing	16
2.2. Multilevel Discrete Wavelet Decomposition	17
2.3. Feature extraction	20
2.4. Support Vector Machine Classifier	20
2.5. Performance assessment	21
<b>3. EXPERIMENTS AND RESULTS</b>	<b>23</b>
3.1. Statistical analysis	24
<b>4. CONCLUSIONS</b>	<b>26</b>
<b>CONTRIBUTIONS</b>	<b>27</b>
<b>BIBLIOGRAPHY</b>	<b>28</b>

## LIST OF FIGURES

	<b>pág.</b>
Figure 1. Preprocessing raw rs-fMRI data using CPAC.	18
Figure 2. Proposed workflow for the classification of autism.	19
Figure 3. Process developed by MDWD to decompose the input signal in two levels.	20
Figure 4. Logistic regression to obtain a single vector of probabilities.	24
Figure 5. ROC curves of the four models.	25

## LIST OF TABLES

	<b>pág.</b>
Table 1. Results obtained by the four models in terms of different performance measures.	24
Table 2. Performance of the models in terms of AUC with 95 % confidence intervals.	25

## RESUMEN

**TÍTULO:** ANÁLISIS COMPUTARIZADO DE MRI PARA EL DIAGNÓSTICO DEL AUTISMO \*

**AUTOR:** WILLIAM ANDRÉS CANCINO REY \*\*

**PALABRAS CLAVE:** AUTISMO, MDWD, rs-fMRI, WAVELET, APRENDIZAJE AUTOMÁTICO.

### DESCRIPCIÓN:

El diagnóstico actual del trastorno del espectro autista es desafiante debido a los complejos síntomas de la enfermedad. Básicamente, este proceso se basa en observaciones puramente conductuales, las cuales lo convierten en un método altamente subjetivo. Además, la presencia de comorbilidades psiquiátricas puede disfrazar o alterar algunos de los síntomas, complicando así la detección del trastorno. Para abordar el problema en cuestión, en este estudio proponemos un enfoque dirigido al diagnóstico automático del autismo que se basa en *Multilevel Discrete Wavelet Decomposition* (MDWD) y Máquinas de Soporte Vectorial (SVM). En primer lugar, utilizamos imágenes de resonancia magnética funcional en estado de reposo (rs-fMRI) del conjunto de datos *Autism Brain Imaging Data Exchange I*, ya que permiten el estudio de posibles anomalías en la conectividad funcional del cerebro asociadas al autismo. Luego, a partir de estas imágenes, extraemos series temporales de regiones de interés definidas por un atlas cerebral. A continuación, aplicamos MDWD a las series temporales y las subseries resultantes se utilizan para la construcción de matrices de conectividad funcional. Finalmente, los vectores de características que se obtienen de estas matrices sirven de entrada al clasificador SVM. El método propuesto se evalúa en 175 secuencias de rs-fMRI. Los resultados muestran que el uso de MDWD en el análisis de las señales proporciona una mejora significativa en el rendimiento del clasificador. Nuestro mejor modelo alcanza una exactitud, precisión y área bajo la curva de 72.5%, 81.3% y 0.788, respectivamente.

---

\* Trabajo de grado

\*\* Facultad de Ingenierías Físico-Mecánicas. Escuela de Ingenierías Eléctrica, Electrónica y Telecomunicaciones. Director: Said Pertuz, PhD.

## ABSTRACT

**TITLE:** COMPUTERIZED ANALYSIS OF MRI FOR THE DIAGNOSIS OF AUTISM \*

**AUTHOR:** WILLIAM ANDRÉS CANCINO REY \*\*

**KEYWORDS:** AUTISM, MDWD, rs-fMRI, WAVELET, MACHINE LEARNING.

### DESCRIPTION:

The current diagnosis of autism spectrum disorder is challenging due to the complex symptoms of the disease. Basically, this process is based on purely behavioral observations, which makes it a highly subjective method. In addition, the presence of psychiatric comorbidities may disguise or alter some of the symptoms, thus complicating the detection of the disorder. To address the problem at hand, in this study we propose an approach aimed at the automatic diagnosis of autism that is based on Multilevel Discrete Wavelet Decomposition (MDWD) and Support Vector Machines (SVM). First, we used resting-state functional magnetic resonance imaging (rs-fMRI) from the Autism Brain Imaging Data Exchange I dataset, as they allow the study of possible abnormalities in functional brain connectivity associated with autism. Then, from these images, we extract time series of regions of interest defined by a brain atlas. Next, we apply MDWD to the time series and the resulting subseries are used for the construction of functional connectivity matrices. Finally, the feature vectors obtained from these matrices serve as input to the SVM classifier. The proposed method is evaluated on 175 rs-fMRI sequences. The results show that the use of MDWD in signal analysis provides a significant improvement in classifier performance. Our best model achieves accuracy, precision and area under the curve of 72.5 %, 81.3 % and 0.788, respectively.

---

\* Bachelor Thesis

\*\* Facultad de Ingenierías Físico-Mecánicas. Escuela de Ingenierías Eléctrica, Electrónica y Telecomunicaciones. Director: Said Pertuz, PhD.



## INTRODUCTION

Autism spectrum disorder (ASD) is a complex and highly heterogeneous neurodevelopmental disorder characterized by deficits in communication and social interaction, restricted activities and interests, and repetitive and stereotyped behavior patterns<sup>1, 2, 3</sup>. According to the World Health Organization, one in 100 children in the world has ASD.

Currently, the gold standard for the diagnosis of autism consists of a behavioral assessment supported by tools such as Autism Diagnostic Interview-Revised (ADI-R)<sup>4</sup> and Autism Diagnostic Observation Schedule-2 (ADOS-2)<sup>5</sup>. However, this procedure is subjective and susceptible to inaccuracies, as it depends largely on the specialist's experience and interpretation of the results obtained. In addition, the presence of psychiatric comorbidities in individuals with autism (e.g., depressive disorders, bipolar disorders, anxiety disorders or schizophrenia) can disguise or alter some

---

<sup>1</sup> *Diagnostic and Statistical Manual of Mental Disorders*. Washington, DC, USA: American Psychiatric Association, 2013.

<sup>2</sup> Tyler C. McFayden y col. "Sex Differences in an Autism Spectrum Disorder Diagnosis: Are Restricted Repetitive Behaviors and Interests the Key?" En: *Review Journal of Autism and Developmental Disorders* 7.2 (ago. de 2019), págs. 119-126.

<sup>3</sup> Suma Jacob y col. "Neurodevelopmental heterogeneity and computational approaches for understanding autism." En: *Translational Psychiatry* 9.1 (feb. de 2019).

<sup>4</sup> Michael Rutter, A Le Couteur y Catherine Lord. "Autism diagnostic interview-revised." En: *Los Angeles, CA: Western Psychological Services* 29.2003 (2003), pág. 30.

<sup>5</sup> Catherine Lord y col. "Autism diagnostic observation schedule, second edition (ADOS-2)." En: *Los Angeles, CA: Western Psychological Corporation* (2012).

symptoms <sup>6, 7</sup>, which increases the complexity of detection. In this way, diagnosis is a long and slow process, lacking neurobiological biomarkers <sup>8</sup>, which may delay early intervention. In fact, accurate and early detection of ASD is fundamental to implement adequate treatments to improve the patient's condition and quality of life <sup>9</sup>.

Recently, machine learning and deep learning (DL) methods trained on structural and functional imaging modalities have become attractive for the diagnosis of psychiatric disorders <sup>10, 11, 12, 13</sup>. Precisely, these studies are shown to be promising candidates that attempt to accelerate, improve and reduce subjectivity in the diagnostic process of autism. Within the different types of neuroimaging data, resting-state functional magnetic resonance imaging (rs-fMRI) is increasingly used and is of particular in-

---

<sup>6</sup> Yvette Hus y Osnat Segal. "Challenges Surrounding the Diagnosis of Autism in Children." En: *Neuropsychiatric Disease and Treatment* Volume 17 (dic. de 2021), págs. 3509-3529.

<sup>7</sup> Laura Fusar-Poli y col. "Missed diagnoses and misdiagnoses of adults with autism spectrum disorder." En: *European Archives of Psychiatry and Clinical Neuroscience* 272.2 (sep. de 2020), págs. 187-198.

<sup>8</sup> Xingdan Liu y Huifang Huang. "Alterations of functional connectivities associated with autism spectrum disorder symptom severity: a multi-site study using multivariate pattern analysis." En: *Scientific Reports* 10.1 (mar. de 2020).

<sup>9</sup> Stephen N. James y Christopher J. Smith. "Early Autism Diagnosis in the Primary Care Setting." En: *Seminars in Pediatric Neurology* 35 (2020), pág. 100827.

<sup>10</sup> Jihoon Oh y col. "Identifying Schizophrenia Using Structural MRI With a Deep Learning Algorithm." En: *Frontiers in Psychiatry* 11 (feb. de 2020).

<sup>11</sup> Atif Riaz y col. "DeepfMRI: End-to-end deep learning for functional connectivity and classification of ADHD using fMRI." En: *Journal of Neuroscience Methods* 335 (abr. de 2020), pág. 108506.

<sup>12</sup> Md Rishad Ahmed y col. "Single Volume Image Generator and Deep Learning-Based ASD Classification." En: *IEEE Journal of Biomedical and Health Informatics* 24.11 (2020), págs. 3044-3054.

<sup>13</sup> Antoine Bernas, Albert P. Aldenkamp y Svitlana Zinger. "Wavelet coherence-based classifier: A resting-state functional MRI study on neurodynamics in adolescents with high-functioning autism." En: *Computer Methods and Programs in Biomedicine* 154 (2018), págs. 143-151.

terest to researchers. This modality is a noninvasive technique that measures brain activity through changes in the blood oxygen level-dependent (BOLD) signal when the subject is in a resting state. In particular, rs-fMRI allows the study of functional connectivity, which examines the temporal correlation between BOLD signals from different brain regions. This concept is a valuable tool, as previous studies have reported alterations associated with autism that manifest as reductions or increases in functional connectivity (FC) <sup>14</sup>.

For the study of rs-fMRI signals in the ASD diagnosis, researchers have adopted different approaches. In <sup>12</sup>, they propose a single volume generator that starts from preprocessed rs-fMRI data and generates two types of brain images: glass brain images and statistical map images. Then, these images serve as input to four classifiers, where each one is composed of a deep learning approach and a customized convolutional neural network. On the other hand, <sup>15</sup> uses 3-dimensional rs-fMRI data and implements a model called DarkASDNet, which is based on the Darknet-19 architecture. DarkASDNet contains 20 convolutional layers and 6 max-pooling layers, and achieves state-of-the-art accuracy during the ASD classification task. In <sup>16</sup>, the first step of the workflow consists of dividing the brain into 200 regions of interest using the Craddock 200 atlas, this in order to reduce the size of the feature vector. Subsequently, they implement two stacked denoising autoencoders for the pre-training stage and a multilayer perceptron for fine tuning.

Previous studies have also explored the use of the wavelet transform on rs-fMRI to

---

<sup>14</sup> Oualid Benkarim y col. "Connectivity alterations in autism reflect functional idiosyncrasy." En: *Communications Biology* 4.1 (sep. de 2021).

<sup>15</sup> Md Shale Ahammed y col. "DarkASDNet: Classification of ASD on Functional MRI Using Deep Neural Network". En: *Frontiers in Neuroinformatics* 15 (2021), pág. 20.

<sup>16</sup> Anibal Sólón Heinsfeld y col. "Identification of autism spectrum disorder using deep learning and the ABIDE dataset". En: *NeuroImage: Clinical* 17 (2018), págs. 16-23.

improve ASD classification. For example, in <sup>17</sup> they take advantage of the temporal dynamics features present in scalogram images, which are constructed from Continuous Wavelet Transform (CWT). In the next stage, these images serve as input to 4 pre-trained deep learning frameworks for feature extraction. Finally, the extracted vectors are input to two different classifiers, SVM and K-Nearest Neighbors. On the other hand, <sup>13</sup> extracts wavelet coherence maps from the time series of socio-executive resting-state networks. Subsequently, the maps are used to obtain a metric called time of in-phase coherence, which describes in-phase and coherent patterns (synchronicity) between pairs of networks. Precisely, this metric is used to train three classifiers based on SVM and Linear Discriminant Analysis. Likewise, <sup>18</sup> introduces a multiclass classification oriented to the diagnosis of ASD subtypes. For this purpose, they determine dynamic FC between brain regions using a novel coherence metric. This metric quantifies the global variability of coherence on specific low-frequency scales of BOLD signals. In this way, they develop a classification algorithm based on convolutional neural networks and wavelet coherence maps of the pairwise regions. In general, DL algorithms can automatically extract features from the raw data through various levels of abstraction. Due to the multilayer representation of the information contained in the input data, where each successive layer extracts increasingly complex features, these methods have achieved revolutionary results <sup>19</sup>, <sup>20</sup>.

---

<sup>17</sup> Mohammed I. Al-Hiyali y col. "Classification of BOLD FMRI Signals using Wavelet Transform and Transfer Learning for Detection of Autism Spectrum Disorder." En: *2020 IEEE-EMBS Conference on Biomedical Engineering and Sciences (IECBES)* (2021), págs. 94-98.

<sup>18</sup> Mohammed Isam Al-Hiyali y col. "Classification of ASD Subtypes Based on Coherence Features of BOLD Resting-state fMRI Signals." En: *2021 International Conference on Intelligent Cybernetics Technology & Applications (ICICyTA)* (2021), págs. 17-22.

<sup>19</sup> Ahmed Sedik y col. "Efficient deep learning approach for augmented detection of Coronavirus disease." En: *Neural Computing and Applications* (ene. de 2021).

<sup>20</sup> Xiao-Ling Zou y col. "A promising approach for screening pulmonary hypertension based on fron-

For this reason, in recent years, DL has been widely used in different fields of science. However, these models are seen as “black box” approaches due to the lack of interpretability, which derives from the inherent complexity in their processes. In this way, a uninterpretable model prevents the extraction of relevant knowledge from the relationships learned by the model itself. Thus, the analysis of data in different frequency bands, which could reveal information of interest, would not be evident by using DL. Precisely because of this problem, we prefer Multilevel Discrete Wavelet Decomposition (MDWD) over DL, since its multiresolution analysis provides an interpretable framework that allows understanding how an unwanted event affects the signal and, subsequently, if required, proposing strategies for its elimination. MDWD is a powerful time-frequency technique used in the analysis of non-stationary signals and allows decomposing an input signal into different levels. Each level contains low and high frequency subseries or contributions.

In addition, a point to highlight is that some of the aforementioned works are based on continuous wavelet transforms (CWTs). Unlike them, we use MDWD, since this methodology provides a minimally redundant representation of a signal. Therefore, the computational resources invested in the calculation and storage of its coefficients are significantly lower than the algorithms based on CWTs. Likewise, MDWD can capture the most important characteristics in a subset of coefficients much smaller than the original signal. This means that this method tends to concentrate the signals in a few large coefficients, while the noise is usually represented by several low magnitude coefficients. This allows the use of easy-to-implement techniques (e.g. statistical thresholding) to eliminate noise-associated components. Moreover, the coefficients obtained by MDWD tend to become decorrelated as the level of reso-

---

tal chest radiographs using deep learning: A retrospective study.” En: *PLOS ONE* 15.7 (jul. de 2020). Ed. por Jie Zhang, e0236378.

lution increases <sup>21</sup>. Precisely, the decorrelated data are relevant in machine learning (ML) because it is desired that each coefficient provides unique information to the model. Thus, having many correlated coefficients can reduce the generalization and predictive ability of the ML model, since they would provide the same information of a common underlying pattern.

Thus, in this work we propose a classification framework based on MDWD and Support Vector Machines (SVM). Initially, MDWD is applied to the time series extracted using a 200-region brain atlas. Then, the resulting subseries or coefficients are used in the feature extraction stage, which is based on the construction of a functional connectivity matrix. Finally, the SVM classifier is trained with the acquired FC features.

---

<sup>21</sup> Abdourrahmane M. Atto, Dominique Pastor y Alexandru Isar. "On the statistical decorrelation of the wavelet packet coefficients of a band-limited wide-sense stationary random process." En: *Signal Processing* 87.10 (oct. de 2007), págs. 2320-2335.

## **1. OBJECTIVES**

### **1.1. General objective**

- To implement a machine learning model for diagnosing autism spectrum disorder from MRI images.

### **1.2. Specific objectives**

1. To adapt a dataset of functional MRI corresponding to a set of patients with ASD and control in order to remove unwanted artifacts.
2. To compare different machine learning algorithms for the analysis of functional MRI.
3. To build the machine learning-based model for ASD diagnosis.
4. To evaluate the final model by means of a cross-validation scheme using the area under ROC curve.

## 2. MATERIALS AND METHODS

### 2.1. Dataset and preprocessing

In our experiments we used rs-fMRI sequences available from the Autism Brain Imaging Data Exchange I (ABIDE I) <sup>22</sup>. ABIDE I is a consortium involving 17 international sites and shares neuroimaging data from 539 subjects with ASD and 573 typically developing controls. Each of these 1112 samples consists of rs-fMRI and structural MRI data, and phenotypic information. In order to avoid confounding due to exogenous variables related to acquisition technologies and the sample population, for this study we considered data from only one site: NYU. This corresponds to 75 patients with ASD and 100 typical controls.

In an effort to reduce the effects of unwanted artifacts and other noise, all 175 images were preprocessed using Configurable Pipeline for the Analysis of Connectomes (CPAC). CPAC belongs to the Preprocessed Connectomes Project (PCP) <sup>23</sup> and provides four preprocessing strategies, which revolve around two approaches. The first approach, global signal regression (GSR), effectively removes global artifacts related to movement and respiration. The second approach consists of band pass filtering (BPF) with lower and upper limits corresponding to 0.01 Hz and 0.1 Hz, respectively. This filtering is used to reduce the effect of very low frequency and high frequency physiological noise. These limits have been established in a frequency range such

---

<sup>22</sup> A. Di Martino and S. Mostofsky. *ABIDE I*. [Online]. Available: [http://fcon\\_1000.projects.nitrc.org/indi/abide/abide\\_I.html](http://fcon_1000.projects.nitrc.org/indi/abide/abide_I.html). 2016.

<sup>23</sup> Craddock Cameron y col. "The Neuro Bureau Preprocessing Initiative: open sharing of preprocessed neuroimaging data and derivatives." En: *Frontiers in Neuroinformatics* 7 (2013).



that spontaneous fluctuations or resting state fluctuations are strongest <sup>24</sup>. Thus, the four strategies are formed by using: the two approaches (BPF+GSR), BPF only, GSR only or none. In addition, all of them include preprocessing steps such as slice time correction, motion realignment, intensity normalization and nuisance signal removal. Figure 1 shows the result of passing the raw rs-fMRI data through the CPAC pipeline. Previously, in <sup>25</sup>, we studied how a specific strategy can affect the classifier behavior. For that reason, we selected the strategy with which the model achieves its best performance, i.e. BPF+GSR. Furthermore, because the preprocessed data correspond to 4-dimensional sequences, 3 spatial and 1 temporal dimensions, it may be inefficient to analyze each voxel of the image. Instead, we divided the brain into 200 regions of interest (ROIs) defined by the Craddock 200 atlas (CC200). In this way, the time series of all voxels within each ROI are extracted and averaged, thus obtaining a single time series per ROI.

## 2.2. Multilevel Discrete Wavelet Decomposition

Multilevel Discrete Wavelet Decomposition (MDWD) is a versatile method used in the analysis of non-stationary signals, which allows extracting time-frequency characteristics from time series. MDWD decomposes a signal into low and high frequency subseries level by level. Therefore, to obtain the subseries of the  $(i+1)$ -th level, MDWD implements two fundamental steps: extraction of intermediate sequences and down-sampling.

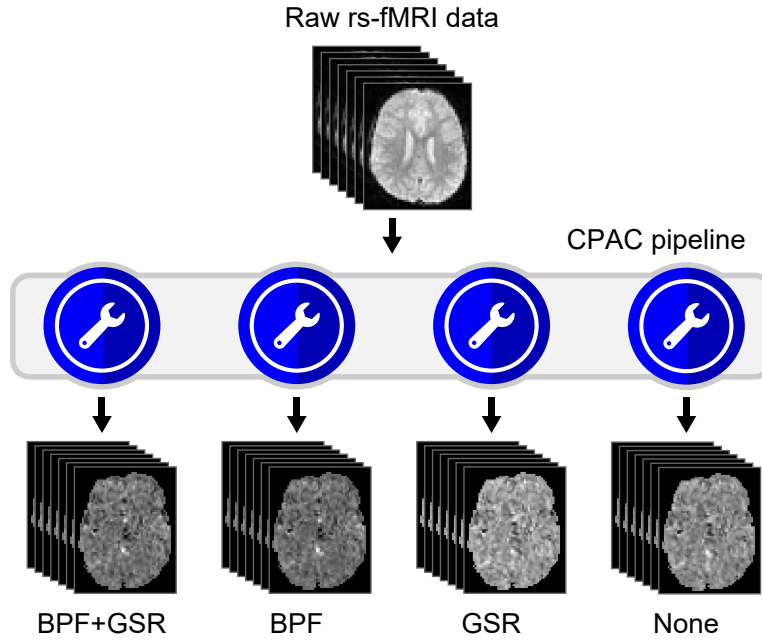
**Extraction of intermediate sequences.** The sequences  $A_{i+1}^l$  and  $A_{i+1}^h$  are genera-

---

<sup>24</sup> Roland Boubela y col. "Beyond Noise: Using Temporal ICA to Extract Meaningful Information from High-Frequency fMRI Signal Fluctuations during Rest". En: *Frontiers in Human Neuroscience* 7 (2013), pág. 168.

<sup>25</sup> William Cancino, Gerson Africano y Said Pertuz. "A Benchmark of Preprocessing Strategies for Autism Classification from Resting-State Functional Magnetic Resonance Imaging". En: *2021 XXIII Symposium on Image, Signal Processing and Artificial Vision (STSIVA)* (2021), págs. 1-5.

Figure 1. Preprocessing raw rs-fMRI data using CPAC.



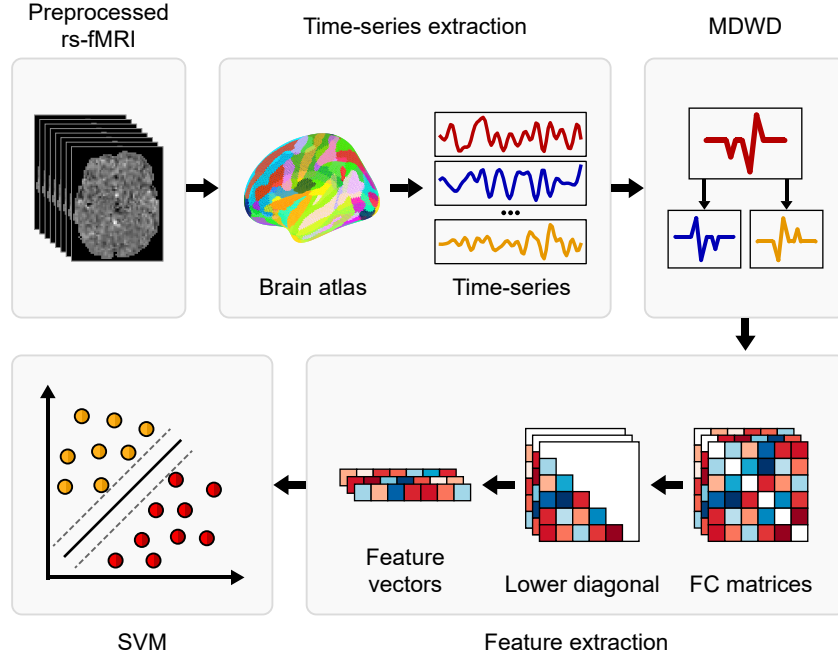
ted by convolving the low-frequency subband of the  $i$ -th level ( $X_i^l$ ) with a low-pass filter  $L = [l_0, l_1, \dots, l_{K-1}]$  and a high-pass filter  $H = [h_0, h_1, \dots, h_{K-1}]$ . Thus, in (1) and (2) the  $n$ -th element of  $A_{i+1}^l$  and  $A_{i+1}^h$  is computed. Additionally, the special case  $X_0^l$  refers to the input time series ( $X$ ).

$$A_{i+1}^l[n] = \sum_{k=0}^{K-1} X_i^l[k] \cdot L[n-k] \quad (1)$$

$$A_{i+1}^h[n] = \sum_{k=0}^{K-1} X_i^l[k] \cdot H[n-k] \quad (2)$$

**Down-sampling.** The low-frequency  $X_{i+1}^l$  and high-frequency  $X_{i+1}^h$  subseries are obtained by applying a decimation function to the  $A_{i+1}^l$  and  $A_{i+1}^h$  sequences, respectively. This process is described by (3) and (4), where  $\downarrow 2(\cdot)$  is the operator that performs down-sampling by a factor of 2.

Figure 2. Proposed workflow for the classification of autism. The overall process starts from the preprocessed rs-fMRI data and ends in the SVM classifier. The intermediate stages correspond to time series extraction, MDWD and feature extraction.

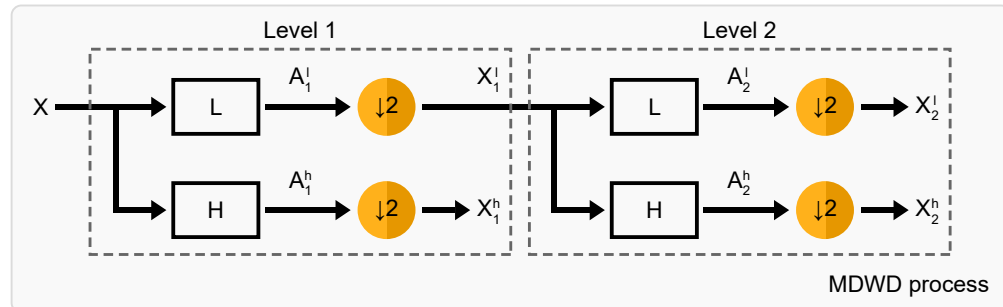


$$X_{i+1}^l = \downarrow 2(A_{i+1}^l) \quad (3)$$

$$X_{i+1}^h = \downarrow 2(A_{i+1}^h) \quad (4)$$

The result of MDWD is a set  $S = [X_1^h, X_2^h, \dots, X_j^h, X_j^l]$  of  $j + 1$  subseries, where  $j$  is the number of levels into which the time series is decomposed. Precisely, the levels used represent the signal viewed at different scales. Finally, in this work we select two decomposition levels ( $j = 2$ ) and use Daubechies 2 to define the coefficients of the  $L$  and  $H$  filters. Furthermore, for each subject we obtain 200 subseries in the first level and 400 subseries in the second level (200 low frequency and 200 high frequency). The decomposition process performed by MDWD is shown in Figure 3.

Figure 3. Process developed by MDWD to decompose the input signal in two levels.



### 2.3. Feature extraction

In this work, we use two levels for the MDWD. As a result, 3 independent functional connectivity matrices are generated for each subject: one for the first level and two for the second level of the MDWD representation of the signal. The FC matrices are of size  $N \times N$  ( $N = 200$ ) and are constructed by calculating Pearson's correlation coefficients for each pair of time subseries. The resulting matrices are symmetric and contain coefficients ranging from 1 (two highly correlated time subseries) to -1 (two anti-correlated time subseries). Subsequently, the elements of the upper diagonal of the FC matrices are discarded, as they are repeated with those of the lower diagonal. Finally, the retained data are reduced to a one-dimensional feature vector of length  $L$ , given by  $L = 0.5N(N - 1)$ . In the same way, the feature extraction process is presented in Figure 2.

### 2.4. Support Vector Machine Classifier

Support Vector Machines (SVM) are a set of supervised machine learning algorithms<sup>26</sup>. SVM develops the classification task by finding a hyperplane that optimally sepa-

<sup>26</sup> Robert Gove y Jorge Faytong. "Machine Learning and Event-Based Software Testing: Classifiers for Identifying Infeasible GUI Event Sequences." En: *Advances in Computers* (2012), págs. 109-135.

rates the data into two classes. This process is performed with the help of support vectors, which are the points in each class that are closest to the hyperplane and influence its orientation and position. Likewise, when the problems are complex, the solutions may require nonlinear hyperplanes. In that case, the original samples of the data set are mapped to a higher dimensional space by a kernel function so that they are now linearly separable. Therefore, in this work we consider the radial basis function (RBF) kernel.

## **2.5. Performance assessment**

For the evaluation of the model we used 5-fold cross validation. Consequently, the data set is divided into 5 folds of the same size, i.e., each containing 35 subjects: 15 with ASD and 20 with typical development (TD). In this way, during the evaluation, a single fold is retained to serve as validation data, and the remaining 4 folds are used as training data. This process is repeated 5 times and each fold is used exactly once to evaluate the model. Similarly, the grid-search method is implemented to find the hyperparameters with which the model achieves the best performance. Therefore, the hyperparameters used for this process correspond to  $C$  and  $\gamma$ , where their intervals are set to  $[10^{-2}, 10]$  and  $[10^{-5}, 10]$ , respectively. The search is performed at each fold using only the training data and 10-fold cross validation.

Likewise, 6 metrics are used to measure classifier performance: accuracy ( $A$ ), precision ( $P$ ), F1-score ( $F1$ ), recall ( $R$ ), specificity ( $S$ ) and area under the curve (AUC) of the receiver operating characteristic (ROC). The first five measures are calculated following the equations (5)-(9), where TP represents the true positives (patients correctly classified with ASD), TN the true negatives (patients correctly classified as TD or without ASD), FP the false positives (patients incorrectly classified with ASD), and FN the false negatives (patients incorrectly classified as TD).

$$A = \frac{TP + TN}{TP + TN + FP + FN} \quad (5)$$

$$P = \frac{TP}{TP + FP} \quad (6)$$

$$R = \frac{TP}{TP + FN} \quad (7)$$

$$F1 = 2 \left( \frac{PR}{P + R} \right) \quad (8)$$

$$S = \frac{TN}{TN + FP} \quad (9)$$

Accuracy measures the ability of a classifier to correctly identify all samples, regardless of whether they are positive or negative. Precision corresponds to the ratio of the number of positive samples correctly predicted to the total number of positive samples predicted. Recall or sensitivity represents the portion of ASD patients correctly classified as ASD. *F1*-score is the harmonic mean of precision and recall. Therefore, this measure considers the impact of false positives and false negatives on the classifier. Thus, the higher the precision and recall, the higher the *F1*-score. Specificity measures the ability of the classifier to correctly determine TD patients. The ROC curve is obtained by plotting the true positive rate against the false positive rate. For this, different values of sensitivity and specificity are previously obtained by varying the decision threshold on the vector of probabilities given by the classifier. Thus, the area under the ROC curve represents the ability of the model to distinguish between classes and its value ranges from zero to one. An AUC of 0.5 means that the model has no discrimination ability, while an AUC of 1.0 means that the classifier is able to distinguish perfectly between true positives and true negatives.

### 3. EXPERIMENTS AND RESULTS

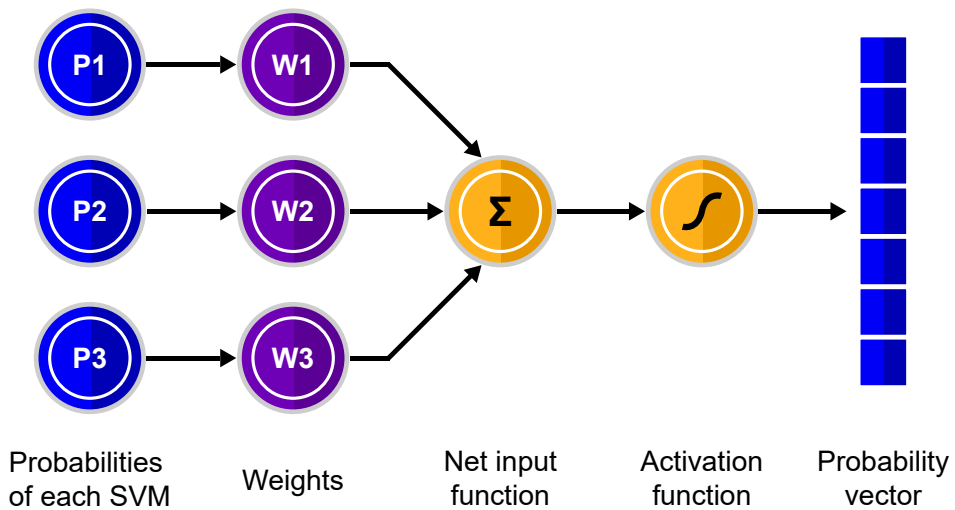
In this work, we want to assess whether the discrimination of ASD from fMRI data has relevant information at different frequency bands. For this reason, we compare the behavior of the model when using or not using the MDWD block. Specifically, for the case where MDWD is added, we explore two options. The first option consists of using data from all decomposition levels. This involves training three different SVM classifiers and then using their probabilities as input features to a logistic regression model, thus obtaining a single vector of probabilities, as shown in Figure 4. The second option considers only the data associated with the low frequency subband of the last level ( $X_2^l$ ). Therefore, Table 1 shows the results of our experiments, where the highest values obtained in each measure are highlighted in bold. We can observe that, for all measurements, the best performances are obtained when using MDWD. This suggests the importance of applying such an algorithm as a method of time series analysis. Also, adding MDWD to our pipeline yields an improvement of up to 5.1 % in terms of accuracy. Similarly, the classifier trained with all levels (All) achieves a precision of up to 81.3 %. On the other hand, evaluating the performance differences between using and not using MDWD, we find that improvements range from 2.6 % to 12.6 %.

In the same way, we evaluate the performance of the state-of-the-art approach proposed in <sup>12</sup>, which is based on a convolutional neural network. For this purpose, the same validation scheme of our method is used and the results are presented in Table 1. In the original work, this architecture achieves an accuracy of 87 % and 88 % when considering stat map and glass brain images, respectively. However, when applying our validation scheme, the performance of the method in question is considerably reduced. Mainly, it can be seen that our framework outperforms the DL model in all performance measures. In fact, the differences in the measures of the

Table 1. Results obtained by the four models in terms of different performance measures.

Model	Measures				
	<i>A</i>	<i>P</i>	<i>F1</i>	<i>R</i>	<i>S</i>
All	<b>0.725</b>	<b>0.813</b>	0.593	0.466	<b>0.920</b>
$X_2^l$	<b>0.725</b>	0.736	<b>0.636</b>	<b>0.560</b>	0.850
No wavelet	0.674	0.687	0.536	0.440	0.850
DL	0.588	0.529	0.428	0.360	0.760

Figure 4. Logistic regression to obtain a single vector of probabilities. The input features correspond to the set of probabilities of three support vector machines.



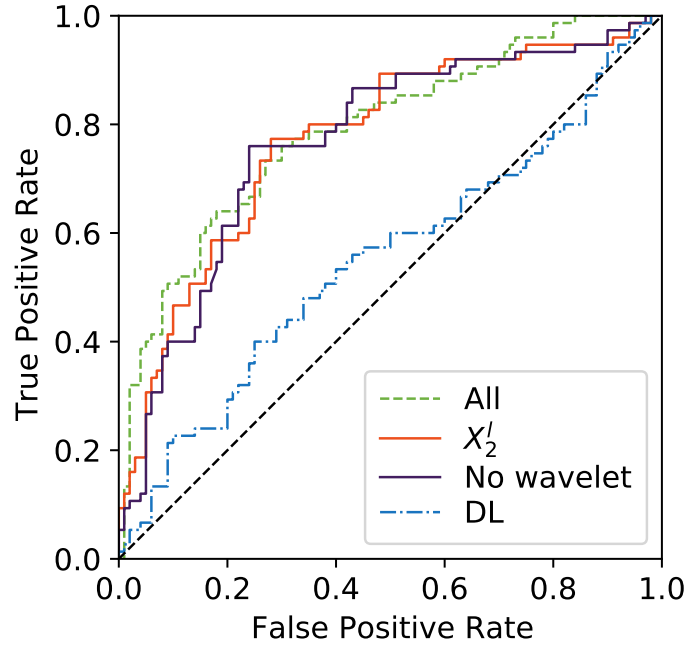
two approaches range from 9% to 28.4%. This highlights the shortcomings of such an approach when considering only data from one site. Moreover, although different DL methods have achieved satisfactory results in ASD classification, the above indicates that there are scenarios where it may be convenient to implement strategies based on traditional machine learning.

### 3.1. Statistical analysis

Likewise, the area under the ROC curve was used to measure the performance of each of the models. In that order, Table 2 reports the AUCs with 95% confidence



Figure 5. ROC curves of the four models.



intervals (CI). These CI were estimated by bootstrapping with replacement. Thus, our method obtains AUCs of 0.788 (All) and 0.773 ( $X_2^l$ ). However, when comparing these values with the AUC of the model without wavelet (0.767) using DeLong’s test, we find that the differences are not statistically significant. On the other hand, the deep learning model obtains a poor AUC of 0.550 (95 % CI: 0.463 - 0.639). The differences between this value and the AUCs of our approach were statistically significant ( $p\text{-value} < 0.05$ ). Additionally, Figure 5 shows the ROC curves of the models in consideration.

Table 2. Performance of the models in terms of AUC with 95% confidence intervals.

Model	AUC
All	<b>0.788 (0.718 - 0.849)</b>
$X_2^l$	0.773 (0.698 - 0.838)
No wavelet	0.767 (0.692 - 0.834)
DL	0.550 (0.463 - 0.639)

## 4. CONCLUSIONS

In this study, we proposed an interpretable approach based on Multilevel Discrete Wavelet Decomposition and SVM for ASD classification. We used 175 rs-fMRI sequences from the ABIDE I dataset and evaluated the model by 5-fold cross validation. Experimental results show an improvement in different performance measures when applying MDWD on time series. This suggests that analyzing the signal in different frequency bands may unveil relevant information that improves classification performance. Also, we compared our method with one of the approaches that has achieved state-of-the-art results in ASD classification. In the end, our model outperformed the reference method. Similarly, the approach we propose in this work may be of particular interest for frameworks that rely on traditional machine learning algorithms, as in many occasions the performance of these methods is limited by the complexity of the raw data. The implemented code is available at <https://github.com/WilliamCancino/autism-degree-project.git>

Future work will utilize the data from all ABIDE I sites and consider the phenotypic information of each subject. In addition, we will adopt an interpretable approach based on deep learning that will allow learning more complex features from the rs-fMRI data and, in turn, provide valuable information to specialists during the autism diagnostic process.

## CONTRIBUTIONS

During the development of this work, the following products were obtained.

### Conference papers

- Cancino, W., Africano, G., & Pertuz, S. (2021). A Benchmark of Preprocessing Strategies for Autism Classification from Resting-State Functional Magnetic Resonance Imaging. In 2021 XXIII Symposium on Image, Signal Processing and Artificial Vision (STSIVA). IEEE. DOI: 10.1109/STSIVA53688.2021.9592011  
Status: Published
- Cancino, W., & Pertuz, S. (2022). Automatic Diagnosis of Autism Using Multilevel Wavelet Decomposition and Support Vector Machine. In X Latin American Congress on Biomedical Engineering (CLAIB 2022) and the XXVIII Brazilian Congress on Engineering Biomedical Engineering (CBEB 2022). Springer International Publishing.  
Status: Accepted

### Collaborations

- Tolonen, A., Pakarinen, T., Sassi, A., Kyttä, J., Cancino, W., Rinta-Kiikka, I., Pertuz, S., & Arponen, O. (2021). Methodology, clinical applications, and future directions of body composition analysis using computed tomography (CT) images: A review. In European Journal of Radiology. Elsevier BV. 145(109943). DOI: 10.1016/J.EJRAD.2021.109943  
Status: Published

## BIBLIOGRAPHY

- A. Di Martino and S. Mostofsky. *ABIDE I*. [Online]. Available: [http://fcon\\_1000.projects.nitrc.org/indi/abide/abide\\_I.html](http://fcon_1000.projects.nitrc.org/indi/abide/abide_I.html). 2016 (vid. pág. 16).
- Ahammed, Md Shale y col. "DarkASDNet: Classification of ASD on Functional MRI Using Deep Neural Network". En: *Frontiers in Neuroinformatics* 15 (2021), pág. 20 (vid. pág. 11).
- Ahmed, Md Rishad y col. "Single Volume Image Generator and Deep Learning-Based ASD Classification." En: *IEEE Journal of Biomedical and Health Informatics* 24.11 (2020), págs. 3044-3054 (vid. págs. 10, 11, 23).
- Al-Hiyali, Mohammed I. y col. "Classification of BOLD fMRI Signals using Wavelet Transform and Transfer Learning for Detection of Autism Spectrum Disorder." En: *2020 IEEE-EMBS Conference on Biomedical Engineering and Sciences (IECBES)* (2021), págs. 94-98 (vid. pág. 12).
- Al-Hiyali, Mohammed Isam y col. "Classification of ASD Subtypes Based on Coherence Features of BOLD Resting-state fMRI Signals." En: *2021 International Conference on Intelligent Cybernetics Technology & Applications (ICICyTA)* (2021), págs. 17-22 (vid. pág. 12).
- Atto, Abdourrahmane M., Dominique Pastor y Alexandru Isar. "On the statistical decorrelation of the wavelet packet coefficients of a band-limited wide-sense stationary random process." En: *Signal Processing* 87.10 (oct. de 2007), págs. 2320-2335 (vid. pág. 14).

- Benkarim, Oualid y col. "Connectivity alterations in autism reflect functional idiosyncrasy." En: *Communications Biology* 4.1 (sep. de 2021) (vid. pág. 11).
- Bernas, Antoine, Albert P. Aldenkamp y Svitlana Zinger. "Wavelet coherence-based classifier: A resting-state functional MRI study on neurodynamics in adolescents with high-functioning autism." En: *Computer Methods and Programs in Biomedicine* 154 (2018), págs. 143-151 (vid. págs. 10, 12).
- Boubela, Roland y col. "Beyond Noise: Using Temporal ICA to Extract Meaningful Information from High-Frequency fMRI Signal Fluctuations during Rest". En: *Frontiers in Human Neuroscience* 7 (2013), pág. 168 (vid. pág. 17).
- Cameron, Craddock y col. "The Neuro Bureau Preprocessing Initiative: open sharing of preprocessed neuroimaging data and derivatives." En: *Frontiers in Neuroinformatics* 7 (2013) (vid. pág. 16).
- Cancino, William, Gerson Africano y Said Pertuz. "A Benchmark of Preprocessing Strategies for Autism Classification from Resting-State Functional Magnetic Resonance Imaging". En: *2021 XXIII Symposium on Image, Signal Processing and Artificial Vision (STSIVA)* (2021), págs. 1-5 (vid. pág. 17).
- Diagnostic and Statistical Manual of Mental Disorders*. Washington, DC, USA: American Psychiatric Association, 2013 (vid. pág. 9).
- Fusar-Poli, Laura y col. "Missed diagnoses and misdiagnoses of adults with autism spectrum disorder." En: *European Archives of Psychiatry and Clinical Neuroscience* 272.2 (sep. de 2020), págs. 187-198 (vid. pág. 10).

- Gove, Robert y Jorge Faytong. "Machine Learning and Event-Based Software Testing: Classifiers for Identifying Infeasible GUI Event Sequences." En: *Advances in Computers* (2012), págs. 109-135 (vid. pág. 20).
- Heinsfeld, Anibal Sólon y col. "Identification of autism spectrum disorder using deep learning and the ABIDE dataset". En: *NeuroImage: Clinical* 17 (2018), págs. 16-23 (vid. pág. 11).
- Hus, Yvette y Osnat Segal. "Challenges Surrounding the Diagnosis of Autism in Children." En: *Neuropsychiatric Disease and Treatment* Volume 17 (dic. de 2021), págs. 3509-3529 (vid. pág. 10).
- Jacob, Suma y col. "Neurodevelopmental heterogeneity and computational approaches for understanding autism." En: *Translational Psychiatry* 9.1 (feb. de 2019) (vid. pág. 9).
- James, Stephen N. y Christopher J. Smith. "Early Autism Diagnosis in the Primary Care Setting." En: *Seminars in Pediatric Neurology* 35 (2020), pág. 100827 (vid. pág. 10).
- Liu, Xingdan y Huifang Huang. "Alterations of functional connectivities associated with autism spectrum disorder symptom severity: a multi-site study using multivariate pattern analysis." En: *Scientific Reports* 10.1 (mar. de 2020) (vid. pág. 10).
- Lord, Catherine y col. "Autism diagnostic observation schedule, second edition (ADOS-2)." En: *Los Angeles, CA: Western Psychological Corporation* (2012) (vid. pág. 9).
- McFayden, Tyler C. y col. "Sex Differences in an Autism Spectrum Disorder Diagnosis: Are Restricted Repetitive Behaviors and Interests the Key?" En: *Review Jour-*

*nal of Autism and Developmental Disorders* 7.2 (ago. de 2019), págs. 119-126 (vid. pág. 9).

Oh, Jihoon y col. "Identifying Schizophrenia Using Structural MRI With a Deep Learning Algorithm." En: *Frontiers in Psychiatry* 11 (feb. de 2020) (vid. pág. 10).

Riaz, Atif y col. "DeepfMRI: End-to-end deep learning for functional connectivity and classification of ADHD using fMRI." En: *Journal of Neuroscience Methods* 335 (abr. de 2020), pág. 108506 (vid. pág. 10).

Rutter, Michael, A Le Couteur y Catherine Lord. "Autism diagnostic interview-revised." En: *Los Angeles, CA: Western Psychological Services* 29.2003 (2003), pág. 30 (vid. pág. 9).

Sedik, Ahmed y col. "Efficient deep learning approach for augmented detection of Coronavirus disease." En: *Neural Computing and Applications* (ene. de 2021) (vid. pág. 12).

Zou, Xiao-Ling y col. "A promising approach for screening pulmonary hypertension based on frontal chest radiographs using deep learning: A retrospective study." En: *PLOS ONE* 15.7 (jul. de 2020). Ed. por Jie Zhang, e0236378 (vid. pág. 12).